

Supporting Information: Optical discrimination of racemic from achiral solutions

Andreas Steinbacher,^a Patrick Nuernberger,^b and Tobias Brixner^{*a}

1 Optical discrimination in the case of a nonlinear dependence on the fs pump-pulse power

As mentioned in the main text, in specific molecular systems, e.g., in chiral photoswitches¹, the assumption that only one fs laser pulse of the pump pulse train triggers a photoreaction might not be valid. In such a case, it might be possible that one photon triggers the first photoreaction while a second one leads to photodecomposition such that one is not operating in the linear power regime. Due to prolonged fs irradiation a further interaction of photoproducts with the fs pump pulse train cannot be excluded. Hence, we discuss the expected signal shapes for photoreactions due to the absorption of two photons from different fs pulses of the pump pulse train theoretically. The special case that those two photons originate from the same fs pulse of the pump pulse train, as e.g. in a nonresonant multiphoton absorption process, is excluded. As will be shown, an optical discrimination between racemic and achiral solutions is not unambiguous, or even impossible, in that case. Although some presented scenarios might be rather unlikely we analyzed all possible pathways in the case of an unknown sample. At first we consider the interaction with LIN polarized fs pump pulses, leading to eight possible scenarios presented in Fig. S1. However, regardless of whether the reactant is achiral (Fig. S1a) or racemic (Fig. S1b), the intermediate as well as the final state can only be a racemic mixture or achiral if LIN polarized pump pulses are utilized. In the following the intermediate state is always generated by the photoreaction triggered by the so-called first photon while the final state is achieved by the absorption of the so-called second photon of the pump pulse train. For example, it might occur that one starts with an achiral solution and generates racemic mixtures with the first (scenario 2 in Fig. S1a) or the first and the second photon (scenario 1.2 in Fig. S1a), but an enantiomeric excess (ee) can never be generated. Also the generation of achiral photoproducts starting from racemic mixtures is possible with only the first (see e.g. scenario 3 in Fig. S1b) or the first and the second photon (see e.g. scenario 4.1 in Fig. S1b), but again the polarimeter would not measure an optical rotation change.

^a Institut für Physikalische und Theoretische Chemie, Universität Würzburg, Am Hubland, 97074 Würzburg, Germany. Fax: +49 931 31-86332; Tel: +49 931 31-86330; E-mail: brixner@phys-chemie.uni-wuerzburg.de

^b Physikalische Chemie II, Ruhr-Universität Bochum, 44780 Bochum, Germany. Tel: +49 234 32-29946; E-mail: patrick.nuernberger@rub.de

The situation changes if one considers circularly polarized pump pulses, presented in Fig. S2. Starting with an achiral molecular system in solution a photoreaction triggered by one photon always leads to no optical rotation change (see scenarios 5 and 6 in Fig. S2a) which was already discussed in the main text. The interaction with the second photon of the circularly polarized fs pump pulse train does not lead to a measurable signal either if the intermediate state is also achiral (confer scenarios 5.1 and 5.2 in Fig. S2a). However, as shown in scenarios 6.1-6.3 in Fig. S2a if the intermediate state is racemic the photoreaction triggered by the second photon leads to signal shapes which are similar to scenario 7 which is presented in Fig. 4 of the main paper. For example scenario 6.2 might be applicable in the case of chiral photoswitches¹. Thus, in general the question arises if it is possible to distinguish between scenario 7 and the scenarios 6.1-6.3 since there is also a non-zero optical rotation change. Furthermore, as presented in Fig. S2b if the initial state is racemic two subsequent photoreactions triggered by the first and the second photon of the circularly polarized pump pulses lead to similar signal shapes as scenario 7. Hence, not only scenarios 6.1 and 6.2 but also scenarios 7.1, 7.2, 8.1, 8.2, 9.1, and 9.2 must be distinguishable for an unambiguous assignment of the underlying photoreaction. Furthermore, as can be seen from the sketched signals in Fig. S2 also the scenarios with an ee as final state (see scenarios 9, 6.3, 8.3, and 9.3 in Fig. S2) must be distinguishable. Thus, we model here all those scenarios theoretically in analogy to the data modeling of the main text. However, the influence of the lock-in amplifier is not included in the simulations for a better comparison of effects arising from the actual molecular system.

Scenarios 8 and 7 can be modeled similarly since for long irradiation times in both cases all molecules in the probe region lead to a zero OA signal. In the first case all molecules are thus converted to the racemate R' after long irradiation which does not deliver an optical rotation change signal. In the latter case all molecules are achiral after long irradiation, also leading to a zero OA signal. Hence, Eq. (4) of the main paper applies also for both, scenario 7 and 8. Furthermore, also scenarios 7.1 and 7.2 can be described analogously since for scenario 7.1 the second interaction does not change the chirality anymore and for scenario 7.2 the second interaction step corresponds to scenario 6, where the polarimeter also cannot detect an optical rotation change. Furthermore, scenarios 6.1

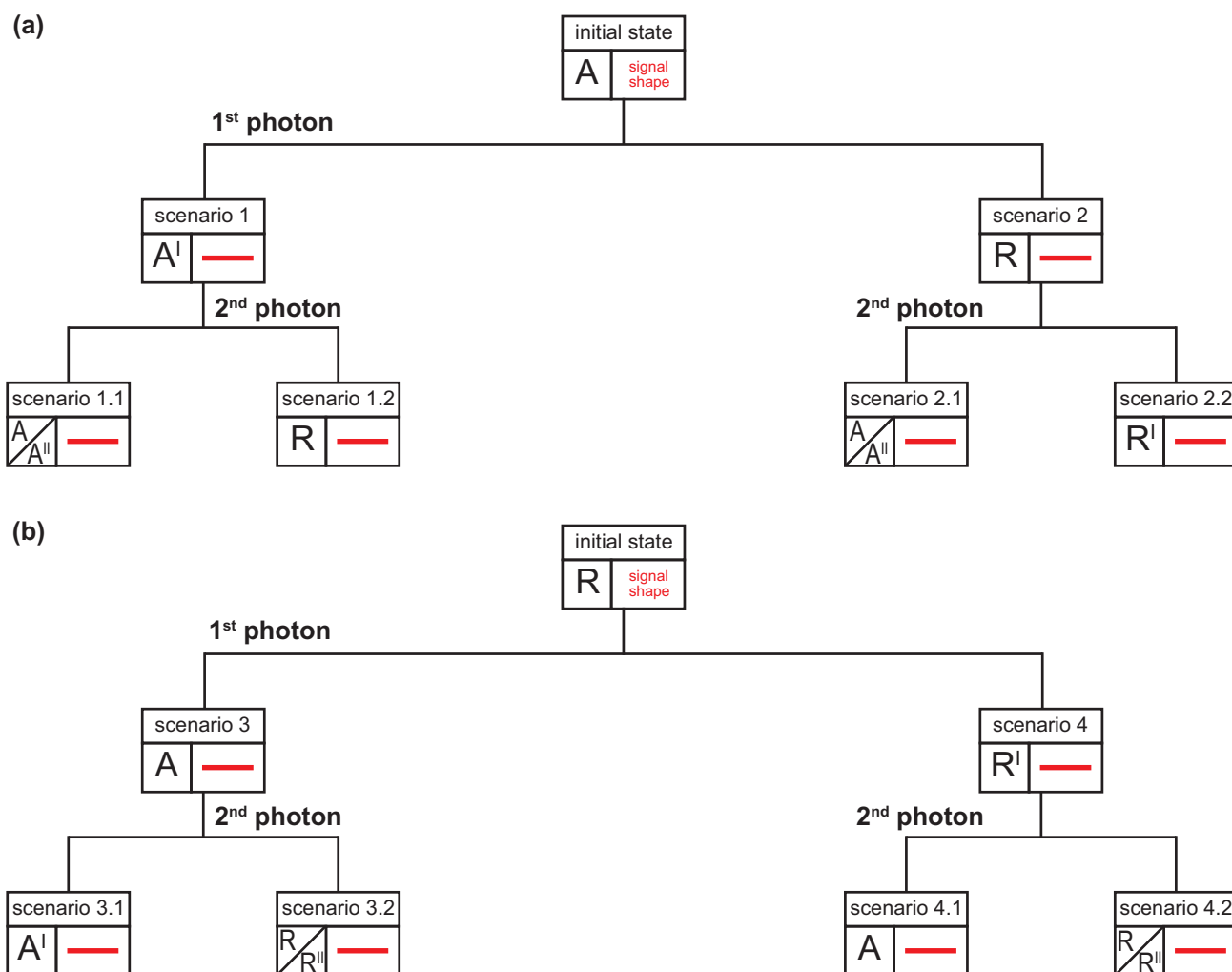


Fig. S1 Schematic representation of the measured optical rotation change for photoreactions triggered by the first and the second photon of the pump pulse train of the unknown solution with LIN polarized fs pump pulses. The signal shape is sketched in red for every scenario. Here, A refers to an achiral molecule which differs from achiral molecules A' and A'' . Analogously R refers to a racemic mixture which differs from the racemates R' and R'' . (a) If the reactant in its initial state is achiral, photochemically only a racemate (scenario 2) or another achiral molecule (scenario 1) can be generated by the first photon, as presented already in Fig. 5a of the main paper. This behavior is similar after the interaction with the second photon (see scenarios 1.1, 1.2 and 2.1, 2.2). Nevertheless, regardless of whether only the first or the first and the second photon trigger the photoreaction, an optical rotation change is never measurable. (b) Starting with a racemate as reactant, again only an achiral sample (scenario 3) or a different racemate R' (scenario 4) is achievable after a photoreaction triggered by the first photon, as presented already in Fig. 5a of the main paper. The subsequent photoreaction triggered by the second photon leads only to racemic mixtures or achiral solutions (see scenarios 3.1, 3.2, 4.1, and 4.2). Hence, independent of whether achiral molecules or racemic mixtures are irradiated with LIN polarized light, no optical rotation change is detected.

and 6.2 can be described by the same equation since in those cases the second photon triggers an analogous photoreaction as in scenarios 7 and 8. With the same reasoning, also scenarios 8.1 and 8.2 can be described with the same equation, as well as scenarios 9.1 and 9.2 can be modeled analogously. Thus, we have performed simulations to compare scenario 7/8, where the photoreaction is triggered only by the first photon,

with scenario 6.1/6.2, scenario 8.1/8.2, and scenario 9.1/9.2, where the first and the second photon trigger two subsequent photoreactions. In all of these cases, the final state is not optically active because it is either achiral or racemic. Furthermore, also scenario 9, where only the first photon triggers a photoreaction, was compared with scenarios 6.3, scenario 8.3, and scenario 9.3, where the first and the second photon trigger

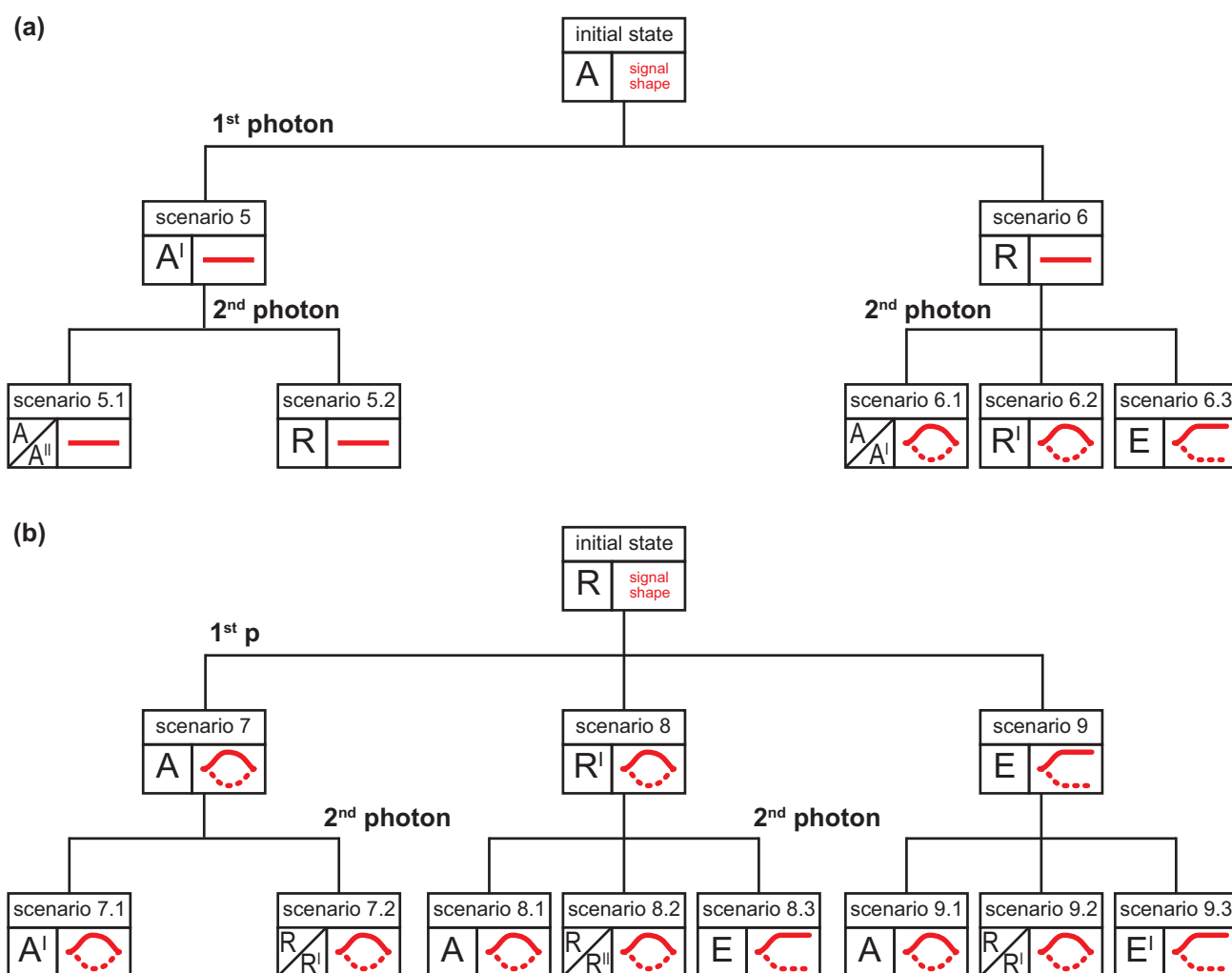


Fig. S2 Schematic representation of the measured optical rotation change for photoreactions triggered by the first and the second photon of the pump pulse train of the unknown solution with circularly polarized (LC or RC) pump pulses. The signal shape is sketched in red (solid and dashed lines refer to the opposite handedness of the circularly pump polarizations) for every scenario. Here, A refers to an achiral molecule which differs from the achiral molecules A' and A''. Analogously R refers to a racemic mixture which differs from the racemates R' and R''. An enantiomeric excess is referred to with the letter E which is different from an ee E'. (a) If the reactant in its initial state is achiral, photochemically only a racemate (scenario 6) or a different achiral molecule A' (scenario 5) can be generated after the photoreaction triggered by the first photon. Hence, no optical rotation change can be observed and the signal corresponds to a flat line as presented already in Fig. 5a of the main paper. This behavior changes if the second photon triggers a further photoreaction starting from the intermediate state. In this case, either again achiral molecules (A, A', A''), racemic mixtures (R, R'), or an ee can be generated. While in scenarios 6.1 and 6.2 the optical rotation change vanishes again (comparable to Fig. 4 of the main paper), for scenario 6.3 a constant signal for prolonged illumination remains. (b) Starting with a racemate as reactant, circularly polarized fs laser pulses can either generate achiral molecules (scenario 7), racemates (scenario 8), or an ee (scenario 9) after a photoreaction triggered by the first photon as presented already in Fig. 5b of the main paper. A subsequent photoreaction due to the second photon of the fs laser pulse train can result in an ee (E, E') if the intermediate is racemic or if an ee is already present (scenarios 8.3 and 9.3). Hence, in these two cases the optical rotation change signal exhibits a constant offset for longer illumination times. Otherwise, either racemic (R, R', R'') or achiral (A, A') solutions are generated which results in signal shapes similar to those of scenarios 7 and 8 where only one photon triggers the photoreaction.

two subsequent photoreactions. Here, the final state is always an enantiomeric excess and thus optically active.

1.1 Optically inactive final state

As mentioned before, the modeling of scenarios 7 and 8 is performed as described in the main text. Hence, we start here

with the theoretical description of scenario 6.1/6.2 where the formation of the intermediate state, a racemic mixture, with the photoreaction triggered by the first photon can be modeled via an additional term in Eq. (3) of the main paper, leading to

$$\frac{dN^R(t)}{dt} = -(\Phi\sigma_{RC}^R + d_{pu})N^R(t) + \frac{1}{2}\Phi N_0\sigma^A \frac{d_{pu} + \Phi\sigma^A e^{-t(d_{pu} + \Phi\sigma^A)}}{d_{pu} + \Phi\sigma^A} \quad (S1)$$

where σ^A refers to the dimensionless cross section of the initially achiral reactant molecules in the solution which get converted to enantiomers. Furthermore, the condition $N^R(t=0) = 0$ must be obeyed since prior to illumination no enantiomers are present. An analogous relation to Eq. (S1) holds for the S-enantiomer (if R is exchanged with S), hence the second term on the right-hand side has a prefactor of $\frac{1}{2}$.

The signal for scenarios 8.1 and 8.2 can be derived via

$$\frac{dN^R(t)}{dt} = -(\Phi\sigma_{RC}^{R2} + d_{pu})N^R(t) + \frac{1}{2}\Phi N_0\sigma_{RC}^R \frac{d_{pu} + \Phi\sigma_{RC}^R e^{-t(d_{pu} + \Phi\sigma_{RC}^R)}}{d_{pu} + \Phi\sigma_{RC}^R} \quad (S2)$$

where σ_{RC}^R refers to the dimensionless cross section for RC light for the reactant R-enantiomer while σ_{RC}^{R2} describes the cross section for RC light for the R-enantiomer of the intermediate racemate R' (compare Fig. S2b). Here, the condition $N^R(t=0) = \frac{1}{2}N_0$ holds since the initial molecular solution is a racemic mixture. An analogous relation to Eq. (S2) holds for the S-enantiomer (if R is exchanged with S).

To be able to model the signal shape of the putative scenarios 9.1 and 9.2 one needs to introduce a new variable k which describes the ee of the intermediate state (confer Fig. S2b). Like an ee [compare Eq. (5) of the main paper] it can range from 0 to 1, corresponding to the range from a racemic mixture to purely one enantiomer, respectively. Together with the dimensionless cross section σ^E the generation of ee can be modeled. Thus, in total scenarios 9.1 and 9.2 can be described by

$$\frac{dN^R(t)}{dt} = -(\Phi\sigma_{RC}^R + d_{pu})N^R(t) + \frac{1-k}{2}\Phi N_0\sigma^E \times \frac{2d_{pu} + (1-k)\Phi\sigma^E e^{-\frac{t}{2}(2d_{pu} + (1-k)\Phi\sigma^E)}}{2d_{pu} + (1-k)\Phi\sigma^E} \quad (S3)$$

An analogous relation to Eq. (S3) holds for the S-enantiomer (if R is exchanged with S). By solving Eqs. (S1), (S2), and (S3) for both enantiomers and calculation of the ee following Eq. (5) of the main paper one arrives at simulated curves as presented in Fig. S3a-d where the three scenarios described above are compared to scenarios 7/8.

By measuring an unknown molecular solution the resulting curves depend on several parameters but in general look very similar, exhibiting a single maximum as presented in Fig. (4) of the main text. Hence, to characterize such curves the time point at which this maximum is achieved and the maximum signal are the two key features of an accumulative OR experiment. Thus, in the following the different scenarios are compared by looking at these two features with respect to a variation of the pump pulse energy. Recording the ee for different pump pulse energies might provide a measure to distinguish scenarios 7/8 from scenarios 6.1/6.2, 8.1/8.2, and 9.1/9.2. Note that also an increase in absorption by a concentration change could be performed instead of a variation of pump-pulse energy, since we always have the product $\Phi\sigma$ in the formulas describing the scenarios. A doubling of the photon flux Φ changes the time point of maximal ee (the optimal time point) for all scenarios depicted in Fig. S3a-d to shorter irradiation times. To elucidate this change quantitatively the behavior of the maximal ee for different Φ values is visualized for scenarios 7/8 and scenarios 6.1/6.2 in Fig. S3e (orange, left axis). Although the absolute values are different, the curve for scenarios 6.1/6.2 is approximately a scaled version of that for scenarios 7/8. Hence, a distinction is not possible by determining the maximal ee for an unknown solution. However, the optimal time point at which the maximal ee is achieved changes differently for scenarios 7/8 and 6.1/6.2 upon varying Φ . This different dependence on Φ is elucidated in Fig. S3e (blue, right axis).

The different behavior of scenarios 7/8 (solid) and 6.1/6.2 (dashed) with respect to variation of Φ is best visualized if the ratio between the maximal ee and the optimal time point, normalized to the value for $\Phi = 1 \times 10^{15}$ photons/s, is plotted. This is shown for various different values of σ^A in Fig. S3f (colored solid lines). If σ^A approaches zero, and is thus significantly smaller than σ_{RC}^R and σ_{LC}^R , it takes infinitely long to populate the intermediate racemate in scenarios 6.1/6.2 [confer Eq. (S1)]. Thus scenarios 6.1/6.2 convert in that case to scenario 5, which can be distinguished since no signal can be recorded by the polarimeter. On the other hand, if σ^A is significantly larger than σ_{RC}^R and σ_{LC}^R , scenarios 6.1/6.2 approach scenarios 7/8, for $t > 0$, since in this case the racemate is formed rapidly via the second term on the right hand side of Eq. (S1). This leads to the same signal shape as for scenarios 7/8 for $\sigma^A = 1 \times 10^{-10}$ and larger values of σ^A . Hence, in Fig. S3f the slope for scenarios 6.1/6.2 approach the black dashed line, representing scenarios 7/8. However, since for an unknown sample one would measure only one slope and is not able to compare to a different case a discrimination is not unambiguously possible in general. Yet, if $\sigma^A \ll \sigma_{RC}^R, \sigma_{LC}^R$, it should be possible to distinguish scenarios 7/8 from 6.1/6.2 since one would even see the delayed rise (see arrow in Fig. S3b) in the measurement signal because

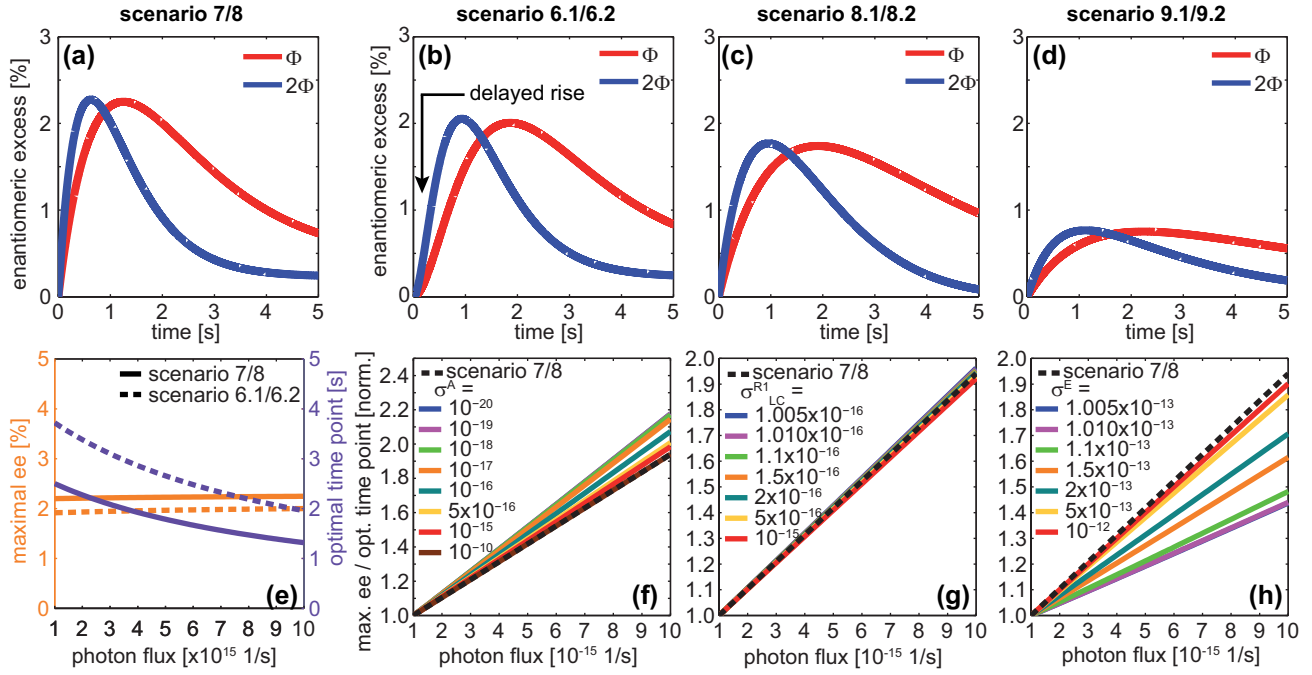


Fig. S3 Simulation of accumulative OR experiments sketched in Fig. S2. Simulation parameters are (comparable to experiment): $N_0 = 3.85 \times 10^{12}$, $\Phi = 2.00 \times 10^{15}$ photons/s, $d_{pu} = 0.0643$ 1/s, $\sigma_{LC}^R = \sigma_{LC}^{R2} = 4.000 \times 10^{-16}$, and $\sigma_{RC}^R = \sigma_{RC}^{R2} = 3.995 \times 10^{-16}$. (a) Dynamical evolution in the case of a racemate according to Eq. (4) of the main paper. The maximal ee value is hardly changed for a doubling of the photon flux Φ , but the maximal ee is achieved earlier. (b) In the case of an achiral solution which is first converted to a racemate with $\sigma^A = 1.00 \times 10^{15}$ from which finally an achiral solution (scenario 6.1) or a different racemate (6.2) is produced in a second step, the solution of Eq. (S1) shows that a doubling of Φ leads to a similar behavior as in scenarios 7/8. However, the time point when the maximal ee is reached is delayed compared to scenarios 7/8 due to the formation of the racemate. (c) If the intermediate racemate is formed with $\sigma_{LC}^R = 1.005 \times 10^{-16}$ and $\sigma_{RC}^R = 1.000 \times 10^{-16}$ from an initially racemic mixture, the dynamical evolution of the maximal ee takes even longer [confer Eq. (S2)]. (d) If the intermediate is an enantiomeric excess ($k = 0.1$) formed with $\sigma^E = 1.0 \times 10^{-16}$ the maximal ee is significantly lower [confer Eq. (S3)]. (e) Dependence of the optimal time point (violet, right axis) and maximal ee value (orange, left axis) on the photon flux Φ for scenarios 7/8 (solid) and 6.1/6.2 (dashed). (f) Ratio between the maximal ee and the optimal time point for different values of σ^A in scenario 6.1/6.2 (solid), normalized to the value for $\Phi = 1 \times 10^{15}$ photons/s. The black dashed line corresponds to scenarios 7/8. (g) Ratio between the maximal ee and the optimal time point for different values of σ_{LC}^R , while $\sigma_{RC}^R = 1.000 \times 10^{-16}$ is kept fixed, in scenario 8.1/8.2 (colored solid), normalized to the value for $\Phi = 1 \times 10^{15}$ photons/s. The black dashed line corresponds to scenarios 7/8. (h) Ratio between the maximal ee and the optimal time point for different values of σ^E ($k = 0.1$ kept fixed) in scenario 9.1/9.2 (colored solid), normalized to the value for $\Phi = 1 \times 10^{15}$ photons/s. The black dashed line corresponds to scenarios 7/8.

the non-zero signal is a consequence of the second interaction only. This effect is already slightly visible in Fig. S3b.

Scenarios 8.1/8.2 are compared to scenarios 7/8 in Fig. S3g. Again, the ratio between the maximal ee and the optimal time point normalized to the value for $\Phi = 1 \times 10^{15}$ photons/s is presented. However, in Fig. S3g the colored solid lines refer to different values for σ_{LC}^R while $\sigma_{RC}^R = 1.000 \times 10^{-16}$ was kept fixed [confer Eq. (S2)]. For the presented parameters, which are of the same magnitude as σ_{RC}^{R2} , σ_{LC}^{R2} a distinction between scenarios 7/8 and 8.1/8.2 is not achievable by comparing the slopes since they do not differ significantly. However, since the initial state of scenario 8.1/8.2 is also chiral and one would observe a comparable signal to scenario 7 (com-

pare Figs. S3a and S3c) one would conclude that a racemic mixture was present in the solution before the experiment, which is indeed true. Even if the cross sections for the first and the second interaction differ significantly (e.g. by several orders of magnitude) a distinction might not be possible by measuring ee kinetics with different pump intensities, since once again only one slope in Fig. S3g would be measured. Note that the parameters were chosen so that the sign of the optical rotation change is identical for the first and the second interaction. If these differed, also a sign change in the observed signal might be visible and thus a distinction would be rather straight-forward. Furthermore, in the case that the absolute values of $\sigma_{LC}^R - \sigma_{RC}^R$ and $\sigma_{LC}^{R2} - \sigma_{RC}^{R2}$ are identical but

the sign differs, no signal is observed at all. This extremely special case thus cannot be resolved.

In the case of scenarios 9.1/9.2 and scenarios 7/8 discrimination might be achieved by measuring ee kinetics with varying pulse energies for the circular polarized pump pulses, as presented in Fig. S3h. As in the two examples before, the ratio between the maximal ee and the optimal time point normalized to the value for $\Phi = 1 \times 10^{15}$ photons/s is plotted. In this case the conversion rate from the initial racemate to the intermeditate enantiomeric excess σ^E is varied while $k = 0.1$ (corresponding to an ee = 0.1) is kept fixed, leading to the colored solid lines in Fig. S3h. If σ^E approaches zero, and is thus significantly smaller than σ_{RC}^R and σ_{LC}^R , it takes infinitely long to populate the intermediate enantiomeric excess in scenarios 9.1/9.2 [confer Eq. (S3)], thus it converts to scenario 7/8 which is represented by the black dashed line in Fig. S3h. On the other hand, if σ^E is significantly larger than σ_{RC}^R and σ_{LC}^R , scenarios 9.1/9.2 approach scenario 9, i.e., a constant offset signal for prolonged illumination can be detected. Hence, this extreme case can be easily distinguished. However, a distinction might not be possible in general. This can be seen from Fig. S3h where the result for various values of σ^E is shown. Again, since in an actual experiment only one slope would be measured and no comparison can be made a distinction is not possible in general. Note that the parameters were chosen that the sign of the optical rotation change is identical for the first and the second interaction. Otherwise, the sign of the optical rotation change signal might again change at a given point in time and thus a distinction is rather straight-forward.

Summing up the simulation results this far, it is possible to distinguish scenarios 7/8 from 6.1/6.2 and from 9.1/9.2, as well as scenarios 6.1/6.2 from 9.1/9.2, for certain parameter ranges if ee kinetics are measured for different pulse energies of the utilized circularly polarized pump pulses. However, in general for an unknown sample an optical discrimination is not possible if two (or even more) subsequent photoreactions within the fs pump pulse train occur. Nevertheless, as mentioned before, the cases where a subsequent photoreaction with a second photon occurs are unlikely such that in the most common case of only one photoreaction optical discrimination of racemic and achiral solutions is always possible.

1.2 Optically active final state

Now we discuss how the distinction between scenario 9 and scenarios 6.3, 8.3, and 9.3 is possible. Again, a possible route is the measurement of ee kinetics with circularly polarized (LC or RC) fs pump pulses and varying the pulse energy. The discrimination of scenario 9 from scenarios 6.3, 8.3, and 9.3 is necessary since the signal shape, as sketched in Fig. S2, can be very similar. Hence, the distinction between scenario 9 and scenario 6.3 is of special interest since here the initial state

is either racemic (scenario 9) or achiral (scenario 6.3). The starting point for our simulations is the defining differential equation for scenario 9, i.e., how a racemate is turned into an ee. This can be described with the help of

$$\frac{dN^R(t)}{dt} = d_{pu} \left(\frac{N_0}{2} - N^R(t) \right) - \frac{1-k}{2} \Phi \sigma^E N^R(t) \quad (S4)$$

where σ^E refers to the dimensionless cross section of the initial racemic mixture which is converted to an ee, described by k . Like an ee [compare Eq. (5) of the main paper] k can range from 0 to 1, corresponding to a racemic mixture or purely one enantiomer, respectively. Since in Eq. (S4) initially a racemic mixture is assumed, the relation $N^R(t=0) = \frac{N_0}{2}$ must hold. An analogous relation to Eq. (S4) holds for the S-enantiomer (if R is exchanged with S).

Scenario 6.3 can be modeled similarly to scenarios 6.1/6.2 [confer Eq. (S1)] where the formation of the racemic mixture with the photoreaction triggered by the first photon can be modeled via an additional term in Eq. (S4). Hence, scenario 6.3 can be described by

$$\begin{aligned} \frac{dN^R(t)}{dt} = & - \left(\Phi \frac{1-k}{2} \sigma^E + d_{pu} \right) N^R(t) \\ & + \frac{1}{2} \Phi N_0 \sigma^A \frac{d_{pu} + \Phi \sigma^A e^{-t(d_{pu} + \Phi \sigma^A)}}{d_{pu} + \Phi \sigma^A} \end{aligned} \quad (S5)$$

where σ^A refers to the dimensionless cross section of the initially achiral molecules in the solution which get converted to enantiomers, constituting the intermediate racemic mixture. The photoreaction triggered by the second photon is characterized in analogy to scenario 9 with σ^E being the dimensionless cross section transferring the intermediate racemate to an ee, which is described by the parameter k . Furthermore, the condition $N^R(t=0) = 0$ must be obeyed since prior to illumination no enantiomers are present in the solution. An analogous relation to Eq. (S5) holds for the S-enantiomer (if R is exchanged with S) so that the second term, populating the intermediate racemate, on the right-hand side has a prefactor of $\frac{1}{2}$.

The signal for scenario 8.3 can be derived in analogy to Eq. (S5), only the first photoreaction now differs for RC and LC light. Hence, the defining differential equation takes the form

$$\begin{aligned} \frac{dN^R(t)}{dt} = & - \left(\Phi \frac{1-k}{2} \sigma^E + d_{pu} \right) N^R(t) \\ & + \frac{1}{2} \Phi N_0 \sigma_{RC}^R \frac{d_{pu} + \Phi \sigma_{RC}^R e^{-t(d_{pu} + \Phi \sigma_{RC}^R)}}{d_{pu} + \Phi \sigma_{RC}^R} \end{aligned} \quad (S6)$$

where σ_{RC}^R refers to the dimensionless cross section for RC light for the starting R-enantiomer. Here, the condition $N^R(t=$

$0) = \frac{1}{2}N_0$ holds since the initial molecular solution is a racemic mixture. Again, the photoreaction triggered by the second photon is characterized in analogy to scenarios 9 and 6.3 with σ^E being the dimensionless cross section transferring the intermediate racemate to an ee, which is described by the parameter k . An analogous relation to Eq. (S6) holds for the S-enantiomer (if R is exchanged with S).

Finally, scenario 9.3 can be modeled by

$$\frac{dN^R(t)}{dt} = -\left(\frac{1-k^{E2}}{2}\sigma^{E2}\Phi + d_{pu}\right)N^R(t) + \frac{1-k^{E1}}{2}\Phi\sigma^{E1} \times \frac{2d_{pu} + (1-k^{E1})\Phi\sigma^{E1}e^{-\frac{1}{2}(2d_{pu}+(1-k^{E1})\Phi\sigma^{E1})t}}{2d_{pu} + (1-k^{E1})\Phi\sigma^{E1}} \quad (S7)$$

where σ^{E1} refers to the dimensionless cross section for conversion of the initial racemate to the intermediate enantiomeric excess E (described by k^{E1}) while σ^{E2} describes the dimensionless cross section for the conversion of the intermediate ee to the final ee E_2 (described by k^{E2}) (compare Fig. S2b). Here, the condition $N^R(t=0) = \frac{1}{2}N_0$ holds since the initial molecular solution is a racemic mixture. An analogous relation to Eq. (S7) holds for the S-enantiomer (if R is exchanged with S). Hence, by solving Eqs. (S4), (S5), (S6), and (S7) for both enantiomers and calculation of the ee following Eq. (5) of the main paper one arrives at simulated curves as presented in Fig. S4 where the four above described scenarios are juxtaposed.

Again, recording the ee dynamics for different pump pulse energies might provide a measure to differentiate scenario 9 from scenarios 6.3, 8.3, and 9.3 as will be discussed in the following. A doubling of the photon flux Φ changes the time point of maximal ee (the optimal time point) for all scenarios depicted in Fig. S4a-d to shorter irradiation times. However, like in the cases of Fig. S3 the change upon higher pump pulse energies must be elucidated quantitatively to assess if a discrimination is possible. Thus, in Fig. S4e (orange, left axis) the behavior of the maximal ee for different Φ values is visualized for scenario 9 and scenario 6.3. Like in Fig. S3e, the optimal time point is presented in Fig. S4e (violet, right axis) for those two scenarios as well. Also in this case a distinction between scenarios 9 and 6.3 is not possible in general if the ee kinetics are measured for different intensities of the circular (LC or RC) polarized pump pulses.

This is seen once more by plotting the ratio between the maximal ee and the optimal time point for different values of σ^A in scenario 6.3 and normalizing to the value for $\Phi = 1 \times 10^{15}$ photons/s (Fig. S4f, colored solid). If σ^A approaches zero, and is thus significantly smaller than σ^E , the formation of the intermediate racemate takes infinitely long in scenario 6.3 [confer Eq. (S5)], thus it converts to scenario 5, which then can be distinguished from scenario 9 since no sig-

nal can be recorded by the polarimeter. On the other hand, if σ^A is significantly larger than σ^E , scenario 6.3 approaches scenario 9, for $t > 0$, since in this case the racemate is formed rapidly via the second term on the right hand side of Eq. (S5). This leads to the same straight line as for scenario 9 (black dashed) in Fig. S4f for $\sigma^A = 1 \times 10^{-10}$ and larger values of σ^A . However, if $\sigma^A \ll \sigma^E$, it should be possible to distinguish scenario 9 from 6.3 since one should even see the delayed rise in the measurement signal. This effect is already slightly visible in Fig. S4b (see arrow).

In analogy to Fig. S4f scenario 8.3 is compared to scenario 9 in Fig. S4g. Again, the ratio between the maximal ee and the optimal time point normalized to the value for $\Phi = 1 \times 10^{15}$ photons/s is presented. However, in Fig. S4g the colored solid lines refer to different values for σ_{LC}^R while $\sigma_{RC}^R = 3.995 \times 10^{-16}$ was kept fixed [confer Eq. (S6)]. As already visible from the exemplary simulated data in Fig. S4c the magnitude of the maximal ee is smaller compared to the other scenarios presented in Fig. S4a,b,d. This is reasonable, since the intermediate racemic mixture must be formed first before the final ee is achieved (see also the delayed rise, marked by an arrow, in Fig. S4c). Nevertheless, for an unknown solution the signal magnitude would also be unknown, thus a distinction must be performed with a different route. Discrimination of scenario 8.3 from scenario 9 might again be possible by measuring with different pump pulse energies as is deducible from the different slopes in Fig. S4g if additional information on possible cross sections and thus the expected slope are known. For greater cross sections $\sigma_{LC}^R, \sigma_{RC}^R$ the maximal ee would rise until in the limiting case of infinite cross sections scenario 8.3 would transfer to scenario 9. Note that here again the parameters were chosen such that the sign of the optical rotation change of the final ee and the intermediate racemate are identical. Otherwise a sign change in the signal would be observable which would make a distinction easier.

Lastly, the case of scenario 9.3 will be discussed. From Fig. S4h, where again the ratio between the maximal ee and the optimal time point normalized to the value for $\Phi = 1 \times 10^{15}$ photons/s is presented, one can already deduce that a distinction is hardly achievable since the slopes of the colored solid lines differ only slightly from the one of scenario 9 (dashed black). In this case the colored solid lines refer to different values of σ^{E1} while $k^{E1} = 0.01$ was kept fixed. For these parameters, which are comparable to σ^{E2} and k^{E2} , a distinction between scenario 9 and 9.3 seems impossible, given the experimental noise of the presented experimental data (confer Fig. 4 of the main paper). Nevertheless, since both the intermediate and the final state correspond to an ee, while the initial state is racemic, such a signal would lead to the correct assignment that the initial sample solution is racemic. Furthermore, the simulation parameters were chosen such that the sign of the simulated optical rotation is identical for both interactions.

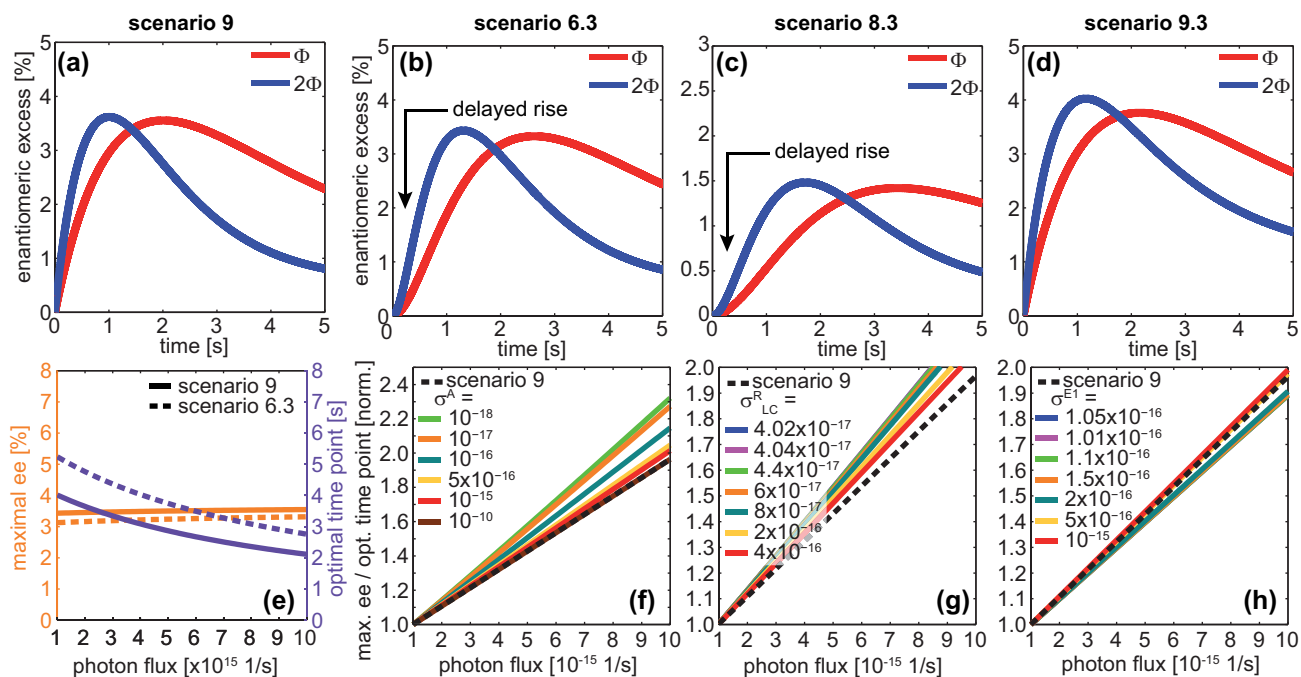


Fig. S4 Simulation of accumulative OR experiments sketched in Fig. S2. Simulation parameters are (comparable to experiment): $N_0 = 3.85 \times 10^{12}$, $\Phi = 2.00 \times 10^{15}$ photons/s, $d_{pu} = 0.0643$ 1/s, $\sigma^E = \sigma^{E2} = 5.000 \times 10^{-16}$, and $k = k^{E2} = 0.1$. (a) Dynamical evolution in the case of a racemate which is converted to an enantiomeric excess according to Eq. (S4). The maximal ee value is hardly changed for a doubling of the photon flux Φ , but the maximal ee is achieved earlier. (b) In the case of an achiral solution which is first converted to a racemate with $\sigma^A = 1.00 \times 10^{15}$ from which an ee is produced in a second step, the solution of Eq. (S5) shows that a doubling of Φ leads to a similar behavior as in scenario 9. However, the optimal time point at which maximal ee is reached is delayed compared to scenario 9 due to the formation of the racemate. (c) If the intermediate racemate is formed with $\sigma_{LC}^R = 1.005 \times 10^{-16}$ and $\sigma_{RC}^R = 1.000 \times 10^{-16}$ from an initially racemic mixture, the dynamical evolution of the maximal ee takes even longer [confer Eq. (S6)]. Furthermore, the achievable maximal ee is significantly lower compared to scenario 9. (d) If the intermediate is an enantiomeric excess ($k = 0.1$) formed with $\sigma^E = 1.0 \times 10^{-16}$ the maximal ee is slightly lowered if the photon flux is doubled. The dynamic evolution can be described via Eq. (S7). However, the signal magnitude and shape is rather comparable to scenario 9. (e) Dependence of the optimal time point (violet, right axis) and maximal ee value (orange, left axis) on the photon flux Φ for scenarios 9 (solid) and 6.3 (dashed). (f) Ratio between the maximal ee and the optimal time point for different values of σ^A in scenario 6.1/6.2 (solid), normalized to the value for $\Phi = 1 \times 10^{15}$ photons/s. The black dashed line corresponds to scenario 9. (g) Ratio between the maximal ee and the optimal time point for different values of σ_{LC}^{R1} , while $\sigma_{RC}^{R1} = 1.000 \times 10^{-16}$ is kept fixed, in scenario 8.3 (colored solid), normalized to the value for $\Phi = 1 \times 10^{15}$ photons/s. The black dashed line corresponds to scenario 9. (h) Ratio between the maximal ee and the optimal time point for different values of σ^{E1} ($k^{E1} = 0.01$ kept fixed) in scenario 9.3 (colored solid), normalized to the value for $\Phi = 1 \times 10^{15}$ photons/s. The black dashed line corresponds to scenario 9.

Otherwise also a sign change in the optical rotation change signal would be detected and thus a distinction would be possible.

Summing up the simulation results for optical discrimination in cases where the final solution is optically active, i.e., an enantiomeric excess, we can conclude that scenarios 6.3 and 8.3 might be distinguishable from scenario 9 by varying the photon flux of the circular polarized fs pump pulses. However, in general a distinction is not possible for an arbitrary unknown solution if several interactions with the fs pump pulse train occur. The same holds in the case of scenario 9.3 where an unambiguous discrimination is not possible except the intermediate and final state are substantially different.

2 Conclusion

Summarizing all results contained in this Supporting Information, an optical discrimination of all possible pathways after two subsequent photoreactions triggered by the first and the second photon of the fs pump pulse train is not possible in general. Hence, if more than one photoreaction takes place for the solutes in the sample volume and the photochemical reaction pathways of the solutes are unknown, ambiguities remain whether the initial solution was achiral or racemic. However, the scenarios discussed in this Supporting Information are far less common than the one-photon scenarios, and still some of them can be distinguished in certain parameter ranges with

our method. The most common case, where the experiment is carried out in a linear power regime and only one photoreaction occurs, is discussed in the main text where distinction of racemic from achiral solutions is always possible.

References

- 1 T. J. Wigglesworth, D. Sud, T. B. Norsten, V. S. Lekhi and N. R. Branda, *J. Am. Chem. Soc.*, 2005, **127**, 7272–7273.